A NON-DESTRUCTIVE PROFILE MONITOR USING A GAS SHEET

N. Ogiwara†, Y. Hikichi, Y. Namekawa, J. Kamiya, M. Kinsho, JAEA, Tokai, Japan
K. Hatanaka, T. Shima, M. Fukuda, RCNP, Osaka, Japan

Abstract

We are developing a dense gas-sheet target to realize a non-destructive and fast-response beam profile monitor for 3 GeV rapid cycling synchrotron (RCS) in the J-PARC. This time, to demonstrate the function of the gas sheet for measuring the 2 dimensional profiles of the accelerated beams, the following experiments were carried out: 1) The gas sheet with a thickness of 1.5 mm and the density of 2×10^{-4} Pa was generated by the combination of the deep slit and the thin slit. Here, the gas sheet was produced by the deep slit, and the shape of the sheet was improved by the thin slit. 2) For the electron beam of 30 keV with a diameter greater than 0.35 mm, the position and the two-dimensional profiles were well measured using the gas sheet. 3) Then the beam position of the 392 MeV proton beam with a current of 1 μA was well measured, too.

INTRODUCTION

A non-destructive and fast-response beam-diagnostic tool for extensive researches has been strongly required in the J-PARC. An idea to realize the fast and non-disruptive beam profile detection is to introduce a gas target so as to increase the interactions with the beam [1-4]. Luminescence lights (or ions) from the target yielded by the collision with the beam are observed. Thus the profile of the beam is obtained. The gas density higher than 10^7 molecules/mm^3 and the thickness of around 1 mm are required for the measurement in the accelerators in the J-PARC. It is essential for realizing the monitor to generate an intense gas target.

Thus, we intended to apply the molecular beam technique for making a compact and large-scale gas-sheet in a vacuum. The molecules emitted from the slit were found to be effectual for making the gas-sheet target unlike capillary [5]. This report will show the outline of the simulation results. Subsequently, the experimental demonstration how the emitted molecules from the deep slit to be useful for detecting the beam will be described.

SIMULATIONS FOR THE DESIGN OF THE GAS SHEET GENERATOR

The test-particle Monte Carlo method in a molecular flow regime is used to determine the angular and density distributions [6,7]. The molecules are assumed to be distributed uniformly and to impinge over the entry plane. Then the molecules are reflected according to the cosine law from the inner wall of the slit. As the outgoing molecules from the slit are able to have the large velocity component parallel to the long side, the slit with the long long-side is seemed to be effectual for making a gas-sheet. Thus calculations for the slit were carried out with the model shown in Fig. 1. The letters a, b, and L represent the lengths of the long and short sides, and the depth of the slit, respectively. The entry and exit planes are A and B, respectively. Origin of Cartesian coordinates (x, y, z) is placed on the center of the plane B and the azimuth λ is also defined as shown in Fig. 1. As the gas-sheet is hoped to be generated on the xy plane, the outgoing molecules with the small angles of λ were mainly examined. After all, it was found that the molecules emitted from the slit can be shaped into a sheet when the following two conditions are satisfied: $L>>b$ *and* $a>>b$. With the parameter set of (L, a, b) = (100, 50, 0.1) (mm), the full width at half maximum (FWHM) of the angular distribution function $n_a(\lambda)$ becomes less than 0.004 rad. The fraction of outgoing molecules collimated within the azimuth $|\lambda|$ of less than 0.01 rad becomes 25% of all molecules [5].

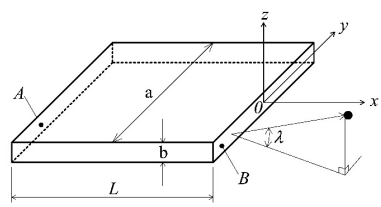

Figure 1: Calculation model.

Then, we calculated the density distribution function $n_d(x, y, z)$. Typical results of the density distribution function $n_d(x, y, z)$ are shown in Fig.2. These are for the slit with the parameter set (L, a, b) = (100, 50, 0.1) (mm). These distribution functions $n_d(x, y, z)$ are plotted as a function of the z coordinate for several parameter sets of (x, y). It is clear that all the curves have the peaks at z=0. This is equivalent to the peaking of $n_a(\lambda)$ at λ=0, and directly shows that the emitted molecules gather on the xy plane. In addition, from these distribution functions, it is found that the gas-sheet density is around 10^{-4} Pa at the point 100 mm away from the exit plane of the generator, when the gas flow rate is 0.1 Paℓ/s. However, the peak height is rather largely reduced with the distance from the exit.

For getting the uniform gas-sheet, it is effectual to superimpose the molecules from some identical slits. We also examined two systems by Monte Carlo simulations. The details were reported elsewhere [8]. One system consists of a thin concentric circular slit with a large aperture. In the case of the circular slit, with inner and outer diameters of 200 and 400 mm, respectively, and a gap of 0.1 mm, the generated gas sheet had a diameter of

†ogiwara.norio@jaea.go.jp

130 mm and the thickness of less than 0.4 mm. The uniformity of the gas density was more than 85%.

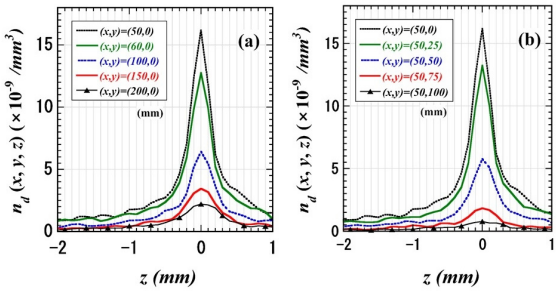

Figure 2: Density distribution function for the deep slit with the parameter set (L, a, b) = (100, 50, 0.1) (mm).

GAS SHEET GENERATOR FOR DEMONSTRATION EXPERIMENTS

According to the above simulations, gas sheet generator for demonstration experiments was constructed as schematically shown in Fig. 3. Main parts of the generator are a deep slit for producing a gas sheet and a thin slit for improving the shape of the sheet. The deep slit, which is formed between 2 SUS304 plates, has a length of 50 mm, a breadth of 0.1 mm, and a depth of 100 mm. A pit with a volume of 4.5 cm^3 for a gas reservoir is also dug adjacent to the thin drain for the deep slit on one of the SUS plates. On the other hand, the thin slit is integrated with the cover of the differential pumping. It is used to control the thickness of the gas sheet. The dimensions are as follows; a length of 60 mm, and a breadth of 0.3 mm. It is set 25 mm apart from the exit surface of the deep slit. Here, we introduce the same coordinates O-xyz as shown in Fig.1 to describe the experimental data of the gas sheet.

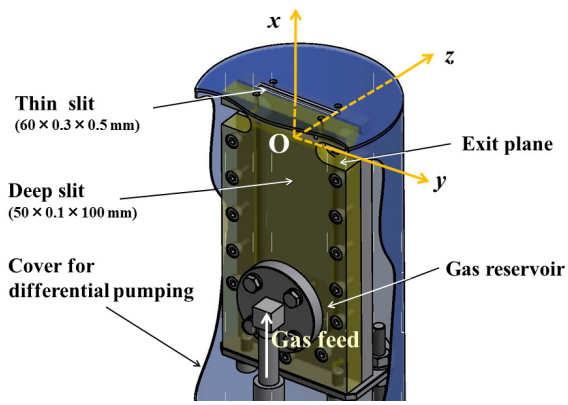

Figure 3: Bird-eye view of the gas sheet generator.

Gas molecules emitted from the gas sheet generator were experimentally studied using a flux monitor. Typical results are shown in Fig. 4(a). Here the inlet gas is Ar. When the head of the flux monitor is moved along the line of (x, y) = (100, 0) (mm), the change in Ar^+ current is measured as a function of z value. Parameter is Ar pressure (P_{Ar}) in the gas reservoir. Most of emitted Ar molecules concentrate on the xy plane. The depth of the gas sheet is evaluated to be 1.5 ± 0.2 mm from the full width of half maximum (FWHM) of the Ar^+ current. The depth is almost independent of the inlet gas pressure.

Then the distribution of the gas density is examined as a function of position using the flux monitor, because the flux is almost proportional to the density in this case. The dependence on y value is plotted on Fig. 4(b), when the flux monitor is moved along the line of (x, z) = (100, 0) (mm). Within a range of $-20 \le y \le 20$ (mm), the gas density has the almost uniform density. The uniformity, which is defined as a rate of minimum to maximum peak current $I(Ar^+)$, is more than 95% within the above range. On the other hand, the density decreases with the distance from the exit plane of the deep slit. An additional technique is needed for achieving uniform density over some area on the xy plane.

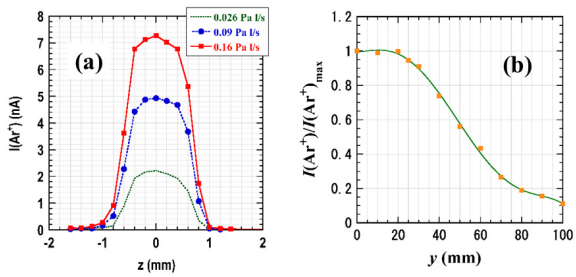

Figure 4: Change in Ar^+ current as a function of the position; (a) dependence on z value, and (b) on y value.

DEMONSTRATION EXPERIMENTS

Detection System

The experimental layout for the electron/proton beam detection with the gas sheet is shown in Fig. 5. The multi-channel plate (MCP) and the fluorescent screen have the same rotational axis, which intersects the electron/proton beam perpendicularly at a point (beam center). The supplementary electrode, which is used to correct the disturbance of the electric field because of the hole on the shield of the MCP, forces the ions generated by the collision of the electron/proton beam with the gas sheet to move toward the MCP in cooperation with the ion repeller. The ions generated by the collision enter the MCP. The secondary electrons due to the ions are amplified through the MCP. Then the fluorescent screen illuminated by the MCP is observed by the CMOS camera through the quartz window. Thus the ions by the collision of the beam with the gas sheet are detected.

The gas sheet is orthogonal to the plane formed by the electron/proton beam and the rotational axis of the MCP. Moreover, the sheet and the electron/proton beam cross each other at a 29.5° angle. As the distance from the beam to the exit plane of the deep slit for generating the gas sheet is 85 mm, the density of the gas sheet is greater than 2×10^{-4} Pa with a pressure of 100 Pa at the gas reservoir.

ISBN 978-3-95450-147-2

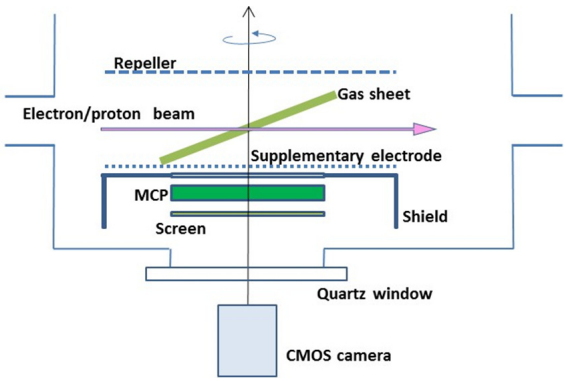

Figure 5: Experimental layout.

Electron Beam Detection

The electron beam is supplied by a commercially available electron gun. Figure 6 shows a photograph of the fluorescent screen illuminated by the MCP during the beam detection experiment using an Ar gas sheet. The bright cigar-shaped spot is caused by ions that are generated by the collision of the electron beam with the gas sheet. The electron beam has a diameter of 0.35 mm and the current of 6 μA. Here, the ambient pressure is 7.8×10^{-6} Pa, where the density of Ar gas sheet is estimated to be around 8×10^{-5} Pa. Thin belt-like trace overlapping with the bright spot is due to the ions generated by the collision of the beam with the uniformly distributed ambient gas.

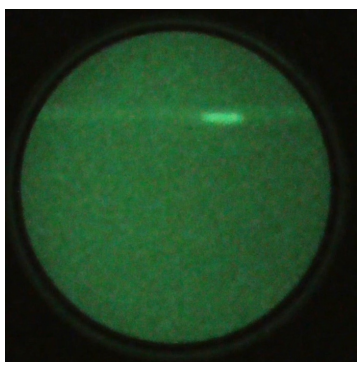

Figure 6: A photograph of the fluorescent screen during electron detection using a gas sheet.

The ion spot is found to move in conjunction with the beam position. In addition, the light intensity of the ion spot is correlated with the gas-sheet density as well as the beam current.

Proton Beam Detection

At the RCNP (Research Center for Nuclear Physics) Cyclotron Facility, Osaka University, we examined the performances of the above detection system, using the 392 MeV proton beam (≤ 1 μA). The details will be reported elsewhere. Here the outline of the results is shown.

Using the graphite foils with a thickness of 25 μm, the vacuum chamber for the detection system had to be isolated from the beam line for maintaining a good vacuum condition. Therefore, there is rather large background noise. The main noise source is secondary radiation, including neutrons and beta and gamma rays, which are generated by the collision of the beam with the foils.

The beam positions were previously measured with the fluorescent screen. Then, the same beam positions are monitored by the detection system with a gas sheet. Beam positions by the fluorescent screen are found to reappear with the detection system, while the 392 MeV beam has the current of 300 nA and over and the diameter of around 2 mm.

Unfortunately, clear beam profiles could not be taken because of the background noise. Extensive investigations are necessary to get a clear profile after reducing the secondary radiation.

SUMMARY

It is essential for realizing the non-destructive profile monitor to generate an intense gas target. Based on the Monte Carlo simulations, we are now developing a new type of gas sheet generator. This time, the following experiments were carried out using this type of generator: 1) Using the electron beam of 30 keV with a diameter greater than 0.35 mm, the position and the two-dimensional profiles were well measured. 2) Then the beam position of the 392 MeV proton beam with the diameter of 2 mm was well monitored.

Above results demonstrate the usefulness of the generator for measuring the 2 dimensional profiles of the accelerated beams.

REFERENCES

[1] B. Vosicki, K. Zankel, IEEE Trans. Nucl. Sci., 22 (1975) 1475.

[2] R. Galiana, D. Manglunki, C. Manzeline, Proc. 1991 IEEE Particle Accelerator Conference, San Francisco, 1991, p. 1198-1200.

[3] A. V. Bubley, V. I. Kudelainen, V. V. Parkhomchuk, B. M. Smirnov, V. S. Tupikov, Proceedings of 17th International Conference on High Energy Accelerators, Dubna, Russia, 1998.

[4] Y. Hashimoto, T. Fujisawa, T. Morimoto, Y. Fujita, T. Honma, S. Muto, K. Noda, Y. Sato, S. Yamada, Nucl. Instrum. Method A, 527 (2004) 289.

[5] N. Ogiwara, and J. Kamiya, J. Vac. Soc. Jpn., 55, (2012) 152-155.

[6] K. Nanbu, Vacuum, 35 (1985) 573.

[7] S. Sukenobu, K. Masaki, K. Ookama, and N. Ogiwara, J. Vac. Soc. Jpn., 56, (2013) 142.

[8] N. Ogiwara, J. Vac. Soc. Jpn., 56, 146-150 (2013).